Analytical Methods

ROYAL SOCIETY OF CHEMISTRY

PAPER
Jae-Hyun Lee *et al.*
Analysis of thermal degradation of bis(2-phenylpyridine)(acetylacetonate)iridium(III) (Ir(ppy)₂(acac)) using spectroelectrochemistry

Indexed in Medline!

Check for updates

Analysis of thermal degradation of bis(2-phenylpyridine) (acetylacetonate)iridium(III) (Ir(ppy)₂(acac)) using spectroelectrochemistry†

Tae-Ho Yang,[a] Hye-Ri Joe,[a] Jin-Seon Heo,[a] Sungmin Kwon,[b] Jonghee Lee [iD] [a] and Jae-Hyun Lee [iD] *[a]

Enhancing the lifespan of organic light-emitting diodes (OLEDs) is crucial for developing stable, high-performance devices. The operational lifetime and performance of OLEDs are reportedly primarily enhanced by the thermal and chemical stability of their constituent single molecules. Therefore, understanding the thermal and electrical stability of these organic molecules is essential for long-lifetime OLED fabrication. However, the degradation of these materials during thermal evaporation has not yet been evaluated. In this study, we investigated the thermal degradation of bis(2-phenylpyridine) (acetylacetonate)iridium(III) (Ir(ppy)₂(acac)), a widely used green phosphorescent dopant, using spectroelectrochemistry (SEC) and matrix-assisted laser desorption/ionization time-of-flight (MALDI-TOF) spectroscopy techniques. SEC measurements revealed the ability of the Ir(ppy)₂(acac) molecules to exhibit different polaron states before and after thermal aging. Gaussian fitting showed the presence of additional polaron absorption peaks in the SEC spectra, which indicated that degradation occurred gradually over the first 4 h of aging and then saturated. MALDI-TOF analysis confirms these results, showing an additional peak at 622.9 *m/z*, corresponding to thermally aged Ir(ppy)₂(acac), alongside the intrinsic molecule peak at 599.8 *m/z*. This result suggested that the Ir(ppy)₂(acac) ligand underwent thermal aging-induced degradation in the deposition chamber. Through this study, we anticipate contributing to related research and industrial advancement by enabling the rapid evaluation of the thermal degradation of OLED materials.

Introduction

Significant advancements have been made in organic light-emitting diodes (OLEDs) to improve their efficiency and stability, with a focus on the synthesis of new materials and optimization of device structures to enhance lifespan and luminous efficiency. Numerous studies have been conducted to extend the lifespan of OLEDs—a critical factor—for commercializing long-lasting products, leading to extensive research.[1,2] These studies have been primarily focused on the synthesis of thermally and electrically stable small molecules or the optimization of OLED device structures based on material properties[3] using optical analysis (such as ultraviolet-visible-near-infrared (UV-vis-NIR) spectroscopy and transient photoluminescence)[4,5] or electro-optical analysis (such as impedance

analysis and transient electroluminescence) techniques.[6,7] Furthermore, molecular-level analyses have been mainly conducted using chromatography, nuclear magnetic resonance spectroscopy, Raman spectroscopy, and matrix-assisted laser desorption/ionization time-of-flight (MALDI-TOF) spectroscopy.[8–12]

In MALDI-TOF spectroscopy (a sophisticated analytical technique), the molecular weight of the components present in a sample are determined by ionizing the sample by laser irradiation and then recording the time required by the ionized sample to reach the detector. A matrix is mixed with the sample to enhance its ionization and reduce fragmentation caused by the laser. MALDI-TOF spectroscopy is widely used for molecular structure analysis owing to its ability for rapid analysis while maintaining accuracy and precision comparable to those of traditional mass spectrometry methods, such as liquid chromatography.

In UV-vis-NIR spectroscopy, which is used to measure the light absorption characteristics of materials, absorption occurs at specific wavelengths owing to electron transition to higher energy states when a molecule absorbs the irradiated light energy. This process reveals the wavelength range of absorption within the UV-vis-NIR spectral range, confirming energy levels

[a] Department of Creative Convergence Engineering, Hanbat National University, 125 Dongseo-daero, Yuseong-gu, Daejeon 34158, South Korea. E-mail: jhyunlee@hanbat.ac.kr

[b] Research Institute of Printed Electronics & 3D Printing, Hanbat National University, 125 Dongseo-daero, Yuseong-gu, Daejeon 34158, Republic of Korea

† Electronic supplementary information (ESI) available. See DOI: https://doi.org/10.1039/d5ay00828j

associated with absorption and emission. It also determines the energy difference between the highest occupied molecular orbital and the lowest unoccupied molecular orbital of a newly synthesized material.[13] When stability analysis results are verified using MALDI-TOF spectroscopy, trace amounts of decomposed molecules may be detected. However, UV-vis-NIR spectrophotometers cannot distinguish the spectral changes caused by such trace amounts of decomposed molecules owing to their limited resolutions. In addition, the peaks corresponding to intrinsic molecules may overlap with the additional absorption peaks originating from such decomposed molecules in the UV-wavelength range. To address these challenges, an electrochemical spectroscopy technique called spectroelectrochemistry (SEC) has been developed,[14,15] in which polarons are generated when a voltage is applied on a sample, and the absorbance can be measured in real time. In the SEC spectrum, the absorption peak associated with intrinsic molecules diminishes and is recorded as a negative value. Consequently, when decomposed molecules generated from thermal reactions or other processes are present in trace quantities, the absorption peak corresponding to the polaron state of the newly formed molecules can be separated within the visible-wavelength range. Thus, compared to traditional UV-vis-NIR methods, SEC allows for a more detailed absorption analysis of polaron states.

Most previous studies on organic molecule degradation have analyzed the changes occurring during device operation or the electrical and thermal degradation observed after fabrication.[4,16,17] However, efficient OLED devices that generate minimal heat during operation undergo thermal degradation primarily during thermal evaporation. Moreover, with the optimization of the mass production process of OLEDs, the thermal deposition process is prolonged for several weeks, potentially accelerating organic molecule degradation. However, the degradation of these materials during the thermal evaporation process remains hitherto unexplored.

In this study, we analyzed the degradation characteristics of Ir(ppy)$_2$(acac) molecules, a light-emitting dopant widely used in green phosphorescent OLEDs, using SEC. Under conditions same as those used in the vacuum chamber for OLED fabrication, thermally degraded Ir(ppy)$_2$(acac) molecules demonstrated additional polaron formation, which manifested as absorption peaks at wavelengths of 305, 338, 422, 495, 935, and 1100 nm in the SEC spectra recorded during the early aging stages. MALDI-TOF analysis confirmed the generation of additional molecules due to aging in thermally degraded samples. This study is expected to promote accurate analyses of organic material degradation under continuous heating conditions that may occur during deposition-assisted mass production of OLEDs.

Results and discussion

Materials and methods

To investigate the effects of thermal degradation on Ir(ppy)$_2$(acac), thermal stress was applied on an OLED evaporator for 1, 2, 4, and 8 h at a temperature of 180 °C, corresponding to a deposition rate of 1 Å s^{-1} for Ir(ppy)$_2$(acac). During this process, the crucible was covered with aluminum foil to prevent sublimation or deposition in the vacuum chamber. To prepare the samples, aliquots were collected at specified time intervals during the thermal treatment.

In the SEC analysis, a potentiostat (CompactStat, IVIUM, Netherlands) was utilized to measure the oxidation potentials of pristine and aged Ir(ppy)$_2$(acac) through cyclic voltammetry (CV) and thus investigate polaron formation. The oxidation potentials (E_{ox}) of small organic molecules were determined by applying a cyclic potential within a specific range, and the voltage at which polaron formation occurred through electrochemical reactions was measured in triplicate at a scan rate of 100 mV s^{-1}. A triple electrode system, consisting of a Pt mesh-type working electrode, a counter electrode, and an Ag/Ag$^+$ reference electrode containing a 0.01 M AgNO$_3$ electrolyte solution, was used. The organic compounds were dissolved at a concentration of 10 mM in anhydrous dichloromethane, and a 0.1 M solution of tetrabutylammonium perchlorate in acetonitrile was used as the electrolyte. The organic emissive-layer material and electrolyte were mixed in a 1 : 1 ratio and placed in a quartz cuvette, which was sealed to prevent concentration changes caused by solvent evaporation. To optically analyze the polaron state, a voltage was applied to the solution samples, and its absorption spectra were measured in the wavelength range of 250–1500 nm using a UV-vis-NIR spectrophotometer (Lambda 1050, PerkinElmer, USA). Before the SEC spectra was measured, a voltage of 1.1 V was applied for 3 min to ensure sufficient polaron formation. To accurately measure small differences in the absorbance spectrum, the spectrum prior to voltage application was used as a baseline, allowing for the detection of spectral changes specifically associated with polaron formation. In addition, Gaussian fitting was performed by the Origin software to identify the absorption peaks corresponding to specific molecules in the SEC spectrum of the degraded sample. For the Gaussian fitting, the underlying principle is as follows: (1) the absorbance spectrum of the sample without applied voltage is used as the baseline measurement, and (2) when a voltage is applied, the molecules transition into polaronic states, resulting in observable changes in the absorbance spectra. To analyze this transition, the absorbance peaks corresponding to neutral molecules were applied as negative peaks in the SEC spectra, indicating a decrease in the density of neutral molecules as polaronic states increase. In this context, the absorbance data from the neutral molecules was defined as Group I. The absorption peak corresponding to polarons generated from neutral (non-degraded) molecules was defined as Group II, while the absorption peak of polarons originating from degraded molecules was designated as Group III. Fig. 1 shows the SEC measurement setup used in this study and a schematic of the Ir(ppy)$_2$(acac) molecule.

Next, MALDI-TOF analysis was performed to identify the decomposed molecules resulting from thermal degradation. For the MALDI-TOF measurements, *trans*-2-[3-(4-*tert*-butylphenyl)-2-methyl-2-propenylidene] malononitrile (DCTB)
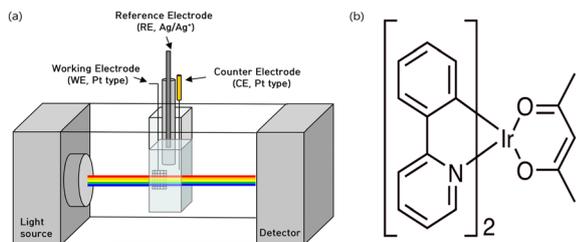
Fig. 1 (a) Measurement setup used in the SEC analysis. (b) Ir(ppy)$_2$(acac) molecule structure.

was used as the matrix material to measure the molecular weights of the molecules.[18,19]

Electrochemical and spectroscopic properties

In the SEC measurements, electrodes were placed in a cuvette with the organic material and electrolyte and an oxidation voltage was applied, followed by performing UV-vis-NIR spectrometry. The absorption peak of intrinsic Ir(ppy)$_2$(acac) was measured as a baseline, and those of the new polaron state Ir(ppy)$_2$(acac)$^+$ were confirmed, as the peak of the neutral molecule in the UV-vis region disappeared upon voltage application. Fig. 2 shows the CV profile used for determining the voltage for polaron formation in Ir(ppy)$_2$(acac), indicating an oxidation voltage at 1.1 V, consistent with that reported in
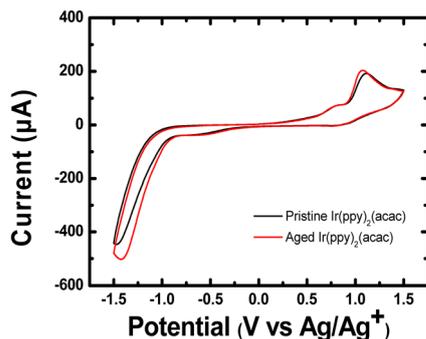
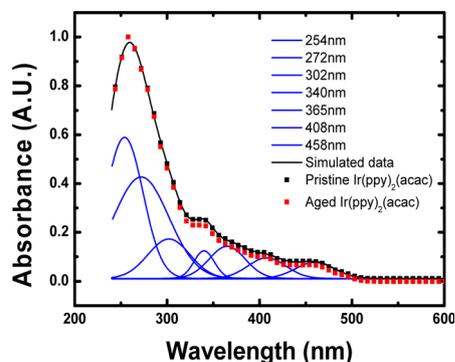previous reports.[20] Because of the absence of significant difference between the CV oxidation peaks of the pristine and aged materials, 1.1 V was applied for the SEC analysis of both the samples.

Fig. 3 demonstrates the UV-vis-NIR spectra of Ir(ppy)$_2$(acac) before and after degradation, showing no significant differences. The well-fitted sum of the Gaussian peaks, represented by the solid black line in Fig. 3, indicates that the spectrum comprises seven sub-Gaussian peaks. These seven peaks, representing the intrinsic absorption peaks of Ir(ppy)$_2$(acac), exhibit negative values in the SEC measurements because the seven absorption peaks of neutral Ir(ppy)$_2$(acac) disappear, while those of the polarons of Ir(ppy)$_2$(acac)$^+$ appear when a voltage is applied.

Fig. 4 depicts the SEC spectra and the corresponding fitting results for Ir(ppy)$_2$(acac) before and after aging. The fitted spectra are categorized into three groups: Group I (solid blue line), Group II (dotted pink line), and Group III (dashed orange line). Group I consists of the seven absorption peaks identified in Fig. 3, corresponding to neutral Ir(ppy)$_2$(acac) molecules observed in the absence of voltage. Upon increasing the applied voltage, the polaron density decreases, resulting in negative absorption values, which indicate that the concentration of neutral Ir(ppy)$_2$(acac) molecules decreases upon voltage application. Conversely, Group II exhibits positive absorption, attributed to the formation of Ir(ppy)$_2$(acac) polarons, which appear with the decreasing concentration of neutral molecules.

This result is confirmed by Fig. 4(b), which shows the SEC spectrum and fitting results for Ir(ppy)$_2$(acac) after 8 h of
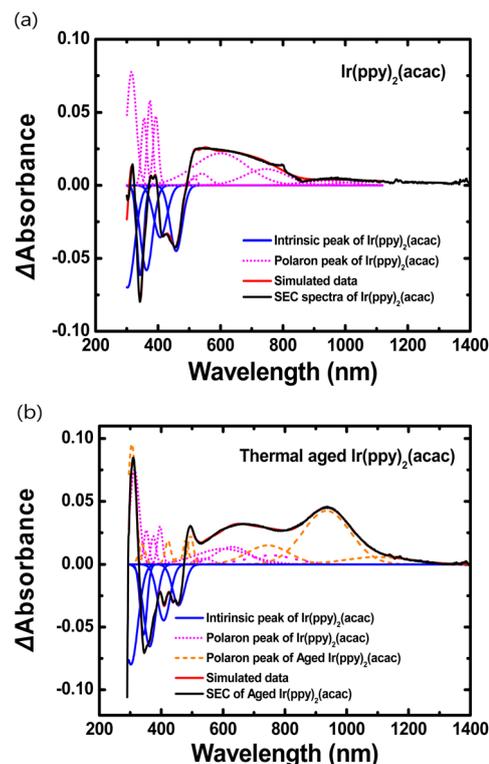

Fig. 2 CV profile of Ir(ppy)$_2$(acac).

Fig. 3 UV-vis spectra and fitting results for pristine and thermally degraded Ir(ppy)$_2$(acac).

Fig. 4 Fitted SEC spectra of (a) Ir(ppy)$_2$(acac) and (b) 8 h thermally aged Ir(ppy)$_2$(acac).

thermal degradation; herein, Groups I and II appear at the same positions. An additional Group III is observed alongside the two groups, corresponding to the polaron peaks associated with molecules newly generated from thermal degradation. This result suggests that prolonged thermal aging causes Ir(ppy)$_2$(-acac) to decompose and recombine, leading to the formation of new molecular species. While discerning thermal aging-induced differences in SEC spectra in the UV range is challenging because of peak overlap, such differences in the visible range can be easily identified. Therefore, the increase in the absorption peak intensity with increasing aging time (Fig. 4(b)) can be attributed to the formation of additional absorption peaks corresponding to the polarons of new molecules generated during the degradation process.

Following the SEC analysis of Ir(ppy)$_2$(acac), MALDI-TOF measurements were conducted to identify the molecules generated by thermal degradation. Because MALDI-TOF measurements can induce additional molecular damage due to laser irradiation during sample ionization, distinguishing this laser-induced damage from thermal aging-induced damage is crucial. During laser ionization, the acac ligand, with the weakest bond, dissociates; consequently, signals corresponding to the 500.8 m/z Ir(ppy)$_2^+$ ion is detected. Peaks at 521.7 and 523.7 m/z are observed, corresponding to the decomposition of phenyl or pyridine group from the phenylpyridine ligand. In addition, the 599.8 m/z Ir(ppy)$_2$(acac)$^+$ ion, consistent with the molecular weight of the original compound, is detected.[19,21] Because similar changes are observed in the aged and nonaged materials, the latter have been excluded from analysis.

Fig. 5 demonstrates that the ratio of a substance, with a molecular weight of 622.9 m/z in the degraded material, increases from 0.04% in the nondegraded state to 0.7% after the degradation. The molecular weight of 622.9 m/z likely represents a new molecular form similar to that of Ir(ppy)(py)(acac)$_2$. This state possibly results from additional bonding between the damaged molecules, such as decomposed pyridine and acac (from ppy and Ir(ppy)$_2$(acac), respectively), owing to thermal degradation. Similar molecular bonding has been observed in previous studies on OLED device degradation, wherein electrical degradation caused ligand separation at the interface, leading to bonding with materials from other device layers.[18] de
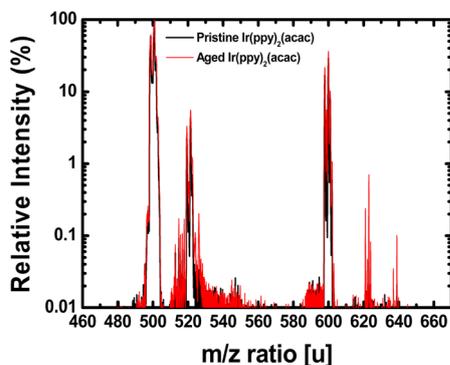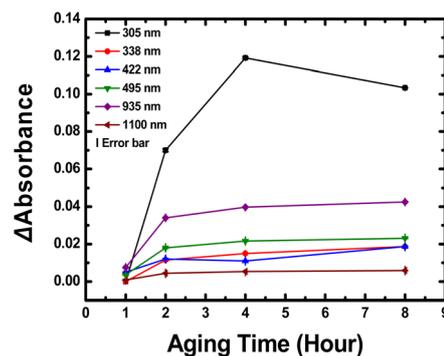

Fig. 6 Fitting results of absorbance measured as a function of degradation time at 305, 338, 422, 495, 935, and 1100 nm.

Moraes *et al.* reported that Ir(ppy)$_2$, a decomposition product of Ir(ppy)$_3$, bonded with the hole-blocking layer BPhen because of electrical degradation, leading to the formation of Ir(ppy)$_2$(-BPhen).[18] These result demonstrate that both thermal and electrical degradation processes can contribute to small-molecule fragment decomposition and recombination.

Ir emitters, with the newly combined ligands, exhibit more complex absorption spectra. Typically, Ir complexes exhibit metal-to-ligand charge transfer (MLCT), ligand-to-ligand charge transfer (LLCT), and intraligand charge transfer (ILCT), which involve charge transfer between the metal and ligand, among different ligands, and within a single ligand, respectively.[22,23] Thus, in addition to the fundamental MLCT transitions in both pristine and aged molecules, the new molecules are expected to exhibit additional absorption peaks originating from LLCT and ILCT transitions from the damaged and modified ligands.[23] Consequently, nine new absorption peaks are identified for Group III. The corresponding data are presented in Table S1 ESI.†

Fig. 6 depicts the intensity of the additional absorption peaks in Group III as a function of aging time. All the detected peaks indicate that absorption increases up to 4 h of aging (degradation time) and then saturates. These results confirm that decomposition from thermal degradation occurs in regions with low bond-dissociation energies, particularly during initial degradation stages.

Conclusions

In this study, we leveraged SEC to investigate the thermal instability of Ir(ppy)$_2$(acac), a green phosphorescent dopant commonly used in OLEDs, subjected to prolonged thermal stress. The dissociation and reformation of specific ligand bonds within the organic molecules resulted in the formation of additional molecules, leading to the emergence of new polaron peaks in the spectra. The absorption spectra of the polaron states of these newly formed molecules were distinguished using SEC. Changes in molecular weights due to degradation were corroborated by MALDI-TOF analyses. The SEC analysis method facilitates the investigation of organic matter in a liquid state, and thus, the amount of sample required for the analysis

Fig. 5 TOF measurement results of Ir(ppy)$_2$(acac) using a DCTB matrix.

is smaller than that required in conventional deposition methods. In addition, changes in material properties can be determined without fabricating a device, allowing for various analyses in a shorter timeframe. Consequently, SEC is anticipated to be beneficial for evaluating the stability of newly synthesized OLED materials and analyzing molecular degradation during OLED fabrication.

Data availability

All data used in the manuscript were produced in our experiments, not from datasets out of our lab. Fig. 1 was drawn in PPT, and Fig. 2–6 were drawn using Origin 8.5 based on Absorbance spectrum data and MALDI-TOF data in our experiments. All data supporting the findings of this study are available in the article.

Author contributions

The manuscript was written through contributions of all authors. All authors have given approval to the final version of the manuscript.

Conflicts of interest

There are no conflicts to declare.

Acknowledgements

Notes and references

1 W. Song and J. Y. Lee, *Adv. Opt. Mater.*, 2017, **5**(9), 1600901.
2 S. S. Swayamprabha, D. K. Dubey, Shahnawaz, R. A. K. Yadav, M. R. Nagar, A. Sharma, F.-C. Tung and J. H. Jou, *Adv. Sci.*, 2021, **8**(1), 2002254.
3 A. Salehi, X. Fu, D. H. Shin and F. So, *Adv. Funct. Mater.*, 2019, **29.15**, 1808803.
4 Y. J. Lim, S. H. Lee, J. Lee, A. Gasonoo and J. H. Lee, *Org. Electron.*, 2022, **104**, 106488.
5 A. S. Sandanayaka, T. Matsushima and C. Adachi, *J. Phys. Chem. C*, 2015, **119**(42), 23845–23851.
6 C. W. Joo, G. Huseynova, J. H. Kim, J. M. Yoo, Y. H. Kim, N. S. Cho, J. H. Lee, Y. H. Kim and J. Lee, *Thin Solid Films*, 2020, **695**, 137753.
7 S. Y. Boo, A. Raji, J. Y. Park, S. Park, J. Lee and J. H. Lee, *J. Inf. Disp.*, 2024, **25**(2), 211–217.
8 H. Pasch and W. Schrepp, *J. Am. Chem. Soc.*, 2003, **125**, 14649–14650.
9 H. Fujimoto, T. Edura, T. Miyayama, N. Sanada and C. Adachi, *J. Vac. Sci. Technol. B*, 2014, **32**(3), 030604.
10 T. Fukushima, J. Yamamoto, M. Fukuchi, S. Hirata, H. H. Jung, O. Hirata, Y. Shibano, C. Adachi and H. Kaji, *AIP Adv.*, 2015, **5**(8), 087124.
11 T. Sugiyama, Y. Furukawa and H. Fujimura, *Chem. Phys. Lett.*, 2005, **405**(4–6), 330–333.
12 S. Scholz, K. Walzer and K. Leo, *Adv. Funct. Mater.*, 2008, **18**(17), 2541–2547.
13 J. C. Costa, R. J. Taveira, C. F. Lima, A. Mendes and L. M. Santos, *Opt. Mater.*, 2016, **58**, 51–60.
14 P. J. Brown, H. Sirringhaus, M. Harrison, M. Shkunov and R. H. Friend, *Phys. Rev.*, 2001, **63**(12), 125204.
15 K. E. Ziemelis, A. T. Hussain, D. D. C. Bradley, R. H. Friend, J. Rühe and G. Wegner, *Phys. Rev. Lett.*, 1991, **66**(17), 2231.
16 G. Huseynova, J. Lee and J. H. Lee, *Mater. Today Energy*, 2021, **21**, 100709.
17 A. Gasonoo, Y. J. Lim, E. J. Jang, J. Lee, M. H. Kim, Y. Choi and J. H. Lee, *Mater. Today Energy*, 2021, **21**, 100794.
18 I. R. de Moraes, S. Scholz and K. Leo, *Org. Electron.*, 2016, **38**, 164–171.
19 X. Lou, J. van Buijtenen, J. J. Bastiaansen, B. F. de Waal, B. M. Langeveld and J. L. van Dongen, *J. Mass Spectrom.*, 2005, **40**(5), 654–660.
20 L. Chen, E. H. Doeven, D. J. Wilson, E. Kerr, D. J. Hayne, C. F. Hogan, W. Yang, T. T. Pham and P. S. Francis, *ChemElectroChem*, 2017, **4**(7), 1797–1808.
21 S. Lamansky, P. Djurovich, D. Murphy, F. Abdel-Razzaq, R. Kwong, I. Tsyba, M. Bortz, B. Mui, R. Bau and M. E. Thompson, *Inorg. Chem.*, 2001, **40**(7), 1704–1711.
22 T. T. Zhang, X. X. Qi, J. Jia and H. S. Wu, *J. Mol. Model.*, 2012, **17**, 4615–4624.
23 J. Li, P. I. Djurovich, B. D. Alleyne, M. Yousufuddin, N. N. Ho, J. C. Thomas, J. C. Peters, R. Bau and M. E. Thompson, *Inorg. Chem.*, 2005, **44**(6), 1713–1727.